Feasibility of incorporating silica aerogel in atmospheric plasma spraying coatings

V. Carnicer*, E. Cañas, M.J. Orts, E. Sánchez

Instituto Universitario de Tecnología Cerámica (IUTC), Universitat Jaume I, 12006, Castellón, Spain

Víctor Carnicer Cervera Telephone number: (+34) 964342424
Email: victor.carnicer@itc.uji.es Fax number: (+34) 964342425

Eugeni Cañas Recacha
Email: eugeni.canas@itc.uji.es

María José Orts Tarí
Email: mariajose.orts@itc.uji.es

Enrique Sánchez Vilches
Email: enrique.sanchez@itc.uji.es

Abstract

This study aims to demonstrate the feasibility of developing zirconia ceramic coatings with the incorporation of silica aerogel particles, which exhibit outstanding insulating properties. Thus, the research aims to find a suitable methodology to disperse aerogel particles, which are strongly hydrophobic, in an aqueous medium. In the study, a double rheological characterisation was carried out, firstly, to adapt the dispersion of the aerogel particles and, secondly, to characterise the different suspensions made up of silica aerogel and zirconia to be atomised. Aerogel additions ranging from 2% to 98% in volume were addressed. Spray-dried powders were characterised in terms of flowability. Finally, coatings microstructure was examined, and their thermal conductivity determined. The results showed that it is possible to disperse aerogel particles in an aqueous medium and to obtain stable suspensions together with the addition of zirconia. Suitable spray-dried powders were then produced in all the cases. On the other hand, coatings obtained by atmospheric plasma spraying showed appreciable microstructural differences with the addition of aerogel particles and their insulating effect is evident in the thermal tests, with their improved (decreased) thermal conductivity.

Keywords: Aerogel, Suspension, Spray-Drying, Thermal Barrier Coating, Atmospheric Plasma Spraying

1. Introduction

Atmospheric plasma spraying (APS) is a technique that has been implemented in industry for decades to obtain thick coatings with very diverse applications that range from protecting metal surfaces against abrasion and corrosion at high temperatures to obtaining bioactive coatings on prostheses for the human body [1,2]. One of the most widespread applications is that of thermal barrier coatings (TBCs) whose purpose is to protect engine and turbine components against corrosion and thermal degradation of combustion gases at very high temperatures [3,4]. Given the importance of this application, research into TBCs has largely grown in last years. This research tries to give answer to the challenges that the turbine engines face at the present time, like increasing the energy efficiency and its time of service. The most used material for making TBCs is yttria partially stabilised tetragonal polycrystalline zirconia (Y–TZP), due to its excellent structural and functional properties: resistance to temperature and corrosion by hot gases, resistance to thermal shock and low thermal conductivity [4–6]. However, the increasing demand for performance and durability to which turbine engines are subjected makes it necessary to continuously improve this type of coating. Thus, in recent years different researchers have developed intense activity based on the addition of other components such as simple (alumina, silica, ceria) or complex oxides (pyrochlores, perovskites or hexaaluminates, among others) that aim to improve the properties of zirconia TBCs, such as increasing their resistance to thermal shock and/or reducing their thermal conductivity [7,8]. With this same objective and maintaining the zirconia composition of TBC, new microstructures have been produced by using liquid feedstocks (suspensions or precursor solutions) in plasma spray [9,10] or multilayer and functionally graded coatings have been prepared [11,12]. More recently, it has been reported that new functionalities can be introduced into TBCs to extend its service life, such as the self-healing function [13,14]. The progress of all this research is more than evident, however, the irruption of a new generation of TBCs to replace all or part of the zirconia coatings is still to come.

A route that has been little explored to date is the use of materials that can contribute to the improvement of the thermal insulation of the coating without significantly compromising the other properties required by the TBC. Thus, aerogels are one of the materials with the highest thermal insulation efficiency, being silica the most common of them all. Silica aerogels are materials with unusual properties, such as an extraordinary specific surface area ($500 \cdot 10^3$–$1000 \cdot 10^3$ $m^2 \cdot kg^{-1}$), ultra-high porosity (around 80 – 99 %),

extremely low density (< 5 $kg \cdot m^{-3}$), very low thermal conductivity (< $5 \cdot 10^{-3}$ $W \cdot m^{-1} \cdot K^{-1}$), ultra-low dielectric constant (between 1 and 2) and a low refractive index (approximately 1.05) [15–19]. This compendium of properties has given rise to intense scientific activity since its discovery back in the 1930s, with a view to developing materials that could be scaled to industry. Thus, a large number of commercial applications in high-tech industries have been documented, such as insulation in thermal windows, acoustic barriers, superconductors or catalytic supports [20–22]. The synthesis of silica aerogel always involves three stages: preparation of the gel, ageing and drying under supercritical conditions. In recent years, the study of the drying process at atmospheric pressure has been intensified, which would greatly facilitate the scaling and marketing of the material [22,23].

The excellent thermal insulation capacity of silica aerogel allows to think about its possible application in thermal spray coatings where this property is of special interest, as for example in TBCs. However, to date, hardly any work has been reported where this approach has been addressed. One of the reasons, could be the enormous difficulty involved in handling a powder with the characteristics described above, which, a priori, cannot be directly fed into a plasma torch. Only some work has been found in which an attempt has been made to mix silica aerogel with other materials to develop suitable powder feedstocks for thermal spray. Applying an experimental design to the atomisation process, *Bheekhun et al.* tried to optimise the atomisation conditions in order to obtain granulated silica powders that could be used in plasma spray. The atomisation was performed using different mixtures of silica aerogel with Y–TZP, obtaining granulated powders that, a priori, could be successfully sprayed, although they did not manufacture coatings with these granulated powders [24]. In a similar work, *Mohd–Zulkifli et al.* dealt with the atomisation of aerogel samples [25], in this case without mixing with any other material, with a view also to their application in thermal spraying coatings, obtaining agglomerated powders that did not spray either. In another investigation [26], these same researchers performed mixtures of aerogel with silica and boron glass microspheres in order to obtain feed powders for plasma spraying with adequate flowability, but they also did not spray them.

From the above, it is concluded that, although silica aerogel seems to have attracted the interest of the scientific community for its use in the manufacture of coatings by thermal

spraying, this interest has not yet materialized in the preparation of coatings, addressing to date only the preparation of the feedstock. The reason is probably, as mentioned above, the enormous difficulty involved in the handling and incorporation of aerogel, either in powder or suspension form, into a thermal spray torch.

Therefore, this research addresses, the reconstitution of silica aerogel and Y–TZP powders by an atomisation process, and, for the first time, the subsequent thermal deposition by atmospheric plasma spraying of the resulting atomised powders. Y–TZP has been chosen as the raw material for mixing with silica aerogel because of the possible application of this material to the preparation of TBCs. The research includes the preparation and characterisation of the aqueous suspensions, the atomisation process, the characterisation of the resulting powders, and deposition and microstructural characterisation of plasma sprayed coatings.

2. Experimental

2.1. Feedstocks preparation and characterisation

A commercial silica aerogel powder supplied by Cabot Speciality Chemicals (Enova® Aerogel IC3100, Cabot Speciality Chemicals, Belgium) was used. Table 1 shows some of the characteristics of this powder according to the information provided by the manufacturer. Micrographs at different magnifications of this material are also shown in Fig. 1. To obtain silica aerogel and zirconia mixtures, a submicron zirconia powder supplied by Tosoh Co. (TZ–3YS, Tosoh Co., Japan), commonly used in TBC coatings, was employed. Some characteristics of this material are also shown in Table 1.

Table 1 Some characteristics of the aerogel IC3100 and TZ – 3YS powder samples used in this research.

Characteristics	**Aerogel IC3100**	**TZ – 3YS**
Size range (m)·10^{-6}	2 – 40	0.1 – 1.4
Density (kg·m^{-3})	120 – 150	6050
Surface area (m^2·kg^{-1}) ·10^{-3}	600 – 800	5 – 9
Thermal conductivity (W·m^{-1}·k^{-1})	0.012 (at 298 K)	2.010 (at 298 K)

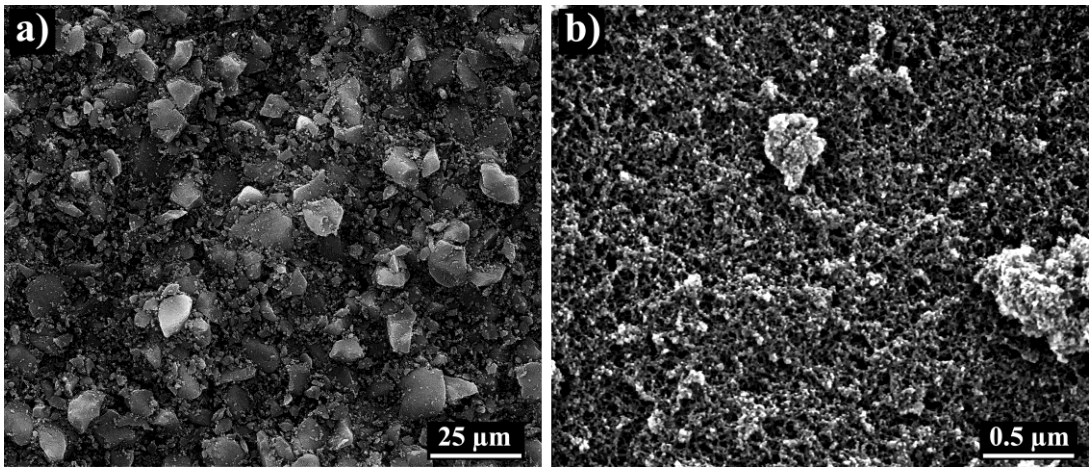

Fig. 1 Micrographs at different magnifications of silica aerogel sample used in the research. a) different silica aerogel particles and b) silica aerogel particle surface.

Initially, a suspension of silica aerogel in water was addressed at 25 vol.%. As the aerogel particles employed in this study display strong hydrophobic character and high specific surface area, a non-ionic surfactant mostly composed of a polyether–modified siloxane (BYK–347, BYK Additives & Instruments, Germany) was used to facilitate the preparation of an aqueous suspension. The surfactant ratio was optimised based on viscosity and surface tension measurements. For that purpose, aliquots of water containing only three different quantities of BYK–347 referred to the amount of water (0%, 1% and 10% all percentages in weight) were prepared and tested with a rotational rheometer (CVO 120, Bohlin Instruments, Great Britain), using a double-gap system and a shear rate of 500 s^{-1}, and a plate-cone tensiometer using the plate element (KRÜSS K12, KRÜSS GmbH, Germany). Once the amount of surfactant has been determined, the suspensions containing only aerogel particles were subjected to different times of sonication in order to evaluate their rheological behaviour for subsequent mixing with Y–TZP powders.

Then, concentrated stable suspensions at 25 vol.% were prepared mixing different proportions of silica aerogel and Y–TZP powders, thus covering coatings in which aerogel particles will act as a minor (dispersed) phase in a Y–TZP matrix against a mixture in which silica aerogel will be the major component (matrix). For comparison purposes, a suspension only with Y–TZP powder was prepared to assess the effect of the aerogel on the coatings. Specifically, the mixtures are detailed in Table 2, as well as the reference of each suspension.

The modus operandi for the preparation of the different mixtures in this work was: first, a stable aqueous Y–TZP suspension was prepared following the route set out in a previous research [27]. Secondly, the optimised amount of BYK-347 was added drop by drop to the stable Y–TZP suspension under mechanical stirring, and finally, the silica aerogel powders were slowly added to the suspension until all ingredients were completely homogenised.

Table 2 Prepared suspensions at 25 vol.% with different proportions of Y–TZP (Z) and silica aerogel (A) powders.

Suspension reference	**Composition of the total solid (vol.%)**	
	Y - TZP	**Silica aerogel**
100Z - 0A	100	-
98Z - 2A	98	2
70Z - 30A	70	30
2Z - 98A	2	98

The suspensions were characterised from the rheological point of view. The rheological study, performed at 298 K and using the same rheometer with the same double – gap system as in the case of the selection of the amount of BYK – 347, was done controlling the shear rate (CR) by loading it from 0 to 500 s^{-1} in 5 min, maintaining the shear rate at 500 s^{-1} for 1 min and downloading it from 500 to 0 s^{-1} in 5 min.

Then, the feedstocks were spray-dried in an atomiser (Mobile Minor, Gea Niro, Denmark) with a drying capacity of 7 kg water/h, in order to obtain reconstituted powders (granules) suitable for its application in plasma spraying. Each feedstock was introduced into the chamber of the atomiser using a pneumatic nozzle at constant flow. The employment of this atomiser implies working in counter current since the nozzle is in the lower part of the chamber and the entry of hot air is made through the upper area of the chamber, thus achieving a longer residence time of the drops in the chamber interior and greater drying efficiency. Concerning the parameters employed for the atomisation step (air flow rate and pressure, feedstock flow rate, inlet gas temperature and nozzle diameter), these were chosen for each suspension based on the height of the droplet column inside the chamber,

so that it reached its maximum height and thus, the residence time of the droplets was as long as possible.

All powders resulting from the atomisation step were characterised in accordance with its size and flowability. The agglomerate size distribution was determined by image analysis software (MicroImage, Olympus Optical Co., Germany). For that purpose, 20 different micrographs of each powder were taken with field emission gun environmental scanning electron microscope (FEG–ESEM, QUANTA 200FEG, FEI Company, USA). Then, the micrographs were treated with the software to determine the total number of agglomerates and its diameter per micrograph to assess the average agglomerate size and the agglomerate size distribution. The micrographs of the atomised powder samples were also employed to analyse their morphology. Likewise, the flowability of the atomised powders was determined from two methods: Hausner ratio test (HR) and angle of repose test (α_M) [28–30]. HR is defined as the quotient of the tapped density (ρ_f) to the bulk (or poured) density of the powder (ρ_o), and as it represents a very simple method (Fig. 2a), it is extensively used in the thermal spraying field [29]. Angle of repose was also determined as a complementary measurement for HR. To determine this parameter, an aliquot of each powder was introduced in a truncated cone plastic container Fig. 2b). Then, the inner part of the container was unlocked, which caused the powder sample to free fall onto a flat and polished metallic surface resulting in a cone of powder. Different runs were done for each powder sample, and for each run several pictures of the powder cone were taken to determine the angle of repose with image analysis software as shown in (Fig. 2b).

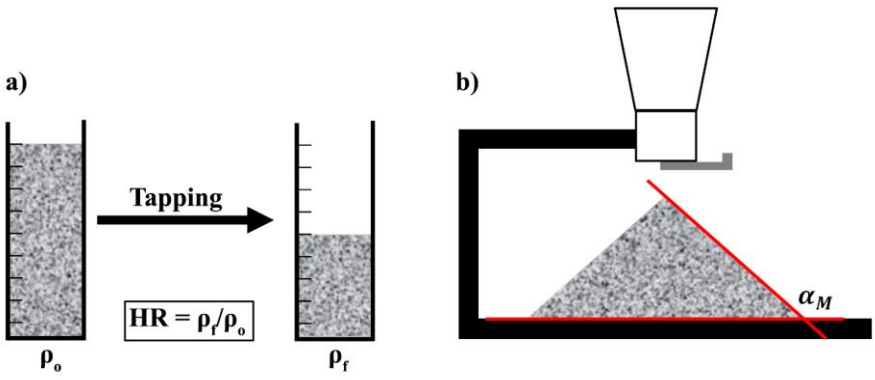

Fig. 2 Diagram of the procedures employed for the characterisation the flowability of the agglomerate powders: a) refers to the Hausner ratio procedure and b) refers to the angle of repose procedure.

2.2. Coatings preparation and characterisation

Once the agglomerated feedstocks were developed and fully characterised, they were plasma sprayed to obtain coatings. The APS facility is comprised by a monocathode plasma torch (F4–MB, Oerlikon Metco, Switzerland), coupled to a six–axis robot (IRB 1400, ABB, Switzerland), which uses argon and hydrogen as primary and secondary plasma gases, respectively. The feeding system is a commercial one (Twin–120A, Oerlikon Metco, Switzerland), in which the powder contained in the hopper is fed into the plasma plume by pneumatic transport using argon as carrier gas.

The substrates used were rectangular sheets of 0.1 x 0.03 m and $3 \cdot 10^{-3}$ m of thickness made of AISI type 304 stainless steel. Prior to the coating deposition process, the surface of the substrates was grit–blasted using black corundum with a pressure of 4.2 bar, until a total surface roughness of approximately 2 μm, and then cleaned with ethanol in an ultrasonic bath. Moreover, an intermediate layer known as bond coat, was sprayed between the substrate and the final coating to enhance its adhesion. The bond coat was deposited by APS from commercial metallic alloy powder (Amdry 997, Oerlikon Metco, Switzerland). The spraying parameters used for its deposition are shown in Table 3 which were given by the supplier. Finally, the different agglomerated powders were sprayed onto the bond coat by APS using the parameters shown in Table 3. These parameters were the same as those employed in the deposition of TBCs from Y–TZP agglomerated powders by APS, extracted from previous research [31,32].

Table 3 Plasma spraying parameters used for the bond coat powder and the spray – dried agglomerates prepared in this research.

Parameters	**Bond coat**	**Z/A agglomerates**
Argon flow rate (slpm*)	65	35
Hydrogen flow rate (slpm*)	8	12
Intensity (A)	650	600
Stand – off distance (m)·10^3	145	80
Traverse robot speed (m·s^{-1})	1	1
Number of scans	2	10
Scan step (m)·10^3	2	4
Nozzle diameter (m)·10^3	1.5	1.8
Carrier gas flow rate (slpm*)	2	3
Powder flow rate (kg·s^{-1})·10^4	6.7	7.5
Preheating (K)	423	-

**slpm: standard litre per minute*

The coatings obtained were inspected with FEG – ESEM on the surface and in cross–section to examine their microstructure. For cross section examination, coatings were cut, mounted in an epoxi resin and polished with different clothes decreasing the grain size of the polishing agent. The resulting cross section micrographs were also employed to estimate the thickness and porosity of the coatings by image analysis (MicroImage). Moreover, qualitative analysis by energy–dispersive X–ray microanalysis (EDX, Genesis 7000 SUTW, EDAX, USA) was performed on different areas of the coatings and the crystalline phases present in the coatings were identified by means of X–ray diffraction (XRD, Advance diffractometer, Bruker Theta – Theta, Germany) using Cu Kα radiation. Furthermore, powder sprayed during the thermal spraying process was collected to determine the chemical composition of the coating. The determination of the chemical composition was performed with a PANalytical model AXIOS X-ray fluorescence wavelength-dispersive spectrometer, with 4 kW power and Rh tube, fitted with flow, scintillation and sealed detectors, and eight analysing crystals: LiF200, LIF220, Ge 111, TLAP, InSb 111-C, PET 002, PX1 and PX7".

Finally, all top coatings were thermally characterised. For this purpose, the thermal conductivity of the coatings for a range of temperatures from 298K to 1273K was calculated through the following equation:

$$\lambda(T) = \alpha(T) \cdot c_p(T) \cdot \rho \text{ (eq. 1)}$$

Where λ is the thermal conductivity ($W \cdot m^{-1} \cdot K^{-1}$), α is the thermal diffusivity ($m^2 \cdot s^{-1}$), c_p the specific heat ($J \cdot kg^{-1} \cdot K^{-1}$) and ρ is the bulk density ($kg \cdot m^{-3}$).

The different parameters of eq. 1 were calculated previously. Thus, thermal diffusivity values were measured with a laser flash equipment (LFA 467 HT Hyperflash, Netzsch, Germany) employing a specific software (Proteus Analysis, Netzsch, Germany). For the measurements, the same procedure described in a previous work [33] has been followed, where some samples with a three layer configuration (substrate, bond coat and ceramic layer) were cut in squares (0.01 x 0.01 m) and covered by a thin layer of graphite aerosol spray to enhance the absorbance and to avoid reflectivity of the surface of metallic substrate. For each temperature, three samples of each coating were tested, and for each combination of sample and studied temperature between 5 and 10 laser beam shots were made, and all findings were averaged.

Concerning the determination of the specific heat, this parameter was measured by means of differential scanning calorimetry (DSC, STA 449C, Netzsch, Germany). For that purpose, each raw material (Y-TPZ and silica aerogel powders) was placed in a platinum crucible inside the DSC. The measurements were carried out in a mixed atmosphere of air and argon. Each raw material was heated from room temperature to 313 K with a heating rate of 3 $K \cdot min^{-1}$, maintained at 313 K for 10 minutes, then taken from 313 K to 1273 K with a heating rate of 5 $K \cdot min^{-1}$ and finally maintained at 1273 K for 10 minutes. The specific heat capacity values of Y–TZP / SiO_2 mixtures at various temperatures were calculated from the rule of mixtures, according to the experimental values of the raw material powders.

Regarding the bulk density of the coating, it was calculated theoretically through equation 2 [33].

$$\rho = \rho_s \cdot (1 - p) \text{ (eq. 2)}$$

Where ρ is the bulk density of the coating ($kg \cdot m^{-3}$), ρ_s is the real density of the solid material ($kg \cdot m^{-3}$) and p is the porosity of the coating. As in the case of the determination of the heat capacity, since the solid material is composed of a mixture of two components, ρ_s was determined by the law of mixtures from the real density of each component, i.e., Y–TZP and silica aerogel.

3. Results and discussion

3.1. Preparation and characterisation of silica aerogel aqueous suspensions

As described above, aerogel particles have a strong hydrophobic character together with a high specific surface area, which increases the difficulty of dispersing such particles in water. Thus, the addition of a surfactant was necessary. Fig. 3 shows the variations in surface tension and viscosity at a shear rate of 500 s^{-1}, as a function of the amount of surfactant added (BYK–347). As can be seen, an addition of 1wt% is sufficient to minimise the surface tension of the water and, at the same time, the viscosity of the mixture remains virtually unchanged, which will favour the wettability of the aerogel particles, while maintaining a low suspension viscosity. For that reason, 1wt% additive will be the proportion used in all experiments. In Fig. 4, the effectiveness of the surfactant was checked with the selected proportion of additive. For this purpose, three different suspensions were prepared, without additive, with additive, and with additive and one minute of sonication (US). The results show the strong hydrophobic character of the aerogel particles (Fig. 4a) which are floating on the water surface hindering the mixing process. The separation between the solid phase and the liquid phase can be clearly seen, since the hydrophobicity of the solid material causes the generation of a thin layer of air at the interface between both materials (water and aerogel particles). In turn, the importance of adding surfactant to promote the wetting of the aerogel particles in water is confirmed, which together with a slight and constant mechanical agitation favours the dispersion of the particles (Fig. 4b), although vigorous mechanical stirring produces the appearance of a surface cream. Finally, the use of sonication seems to promote the incorporation of air bubbles into suspension easily (Fig. 4c), as well as vigorous mechanical stirring.

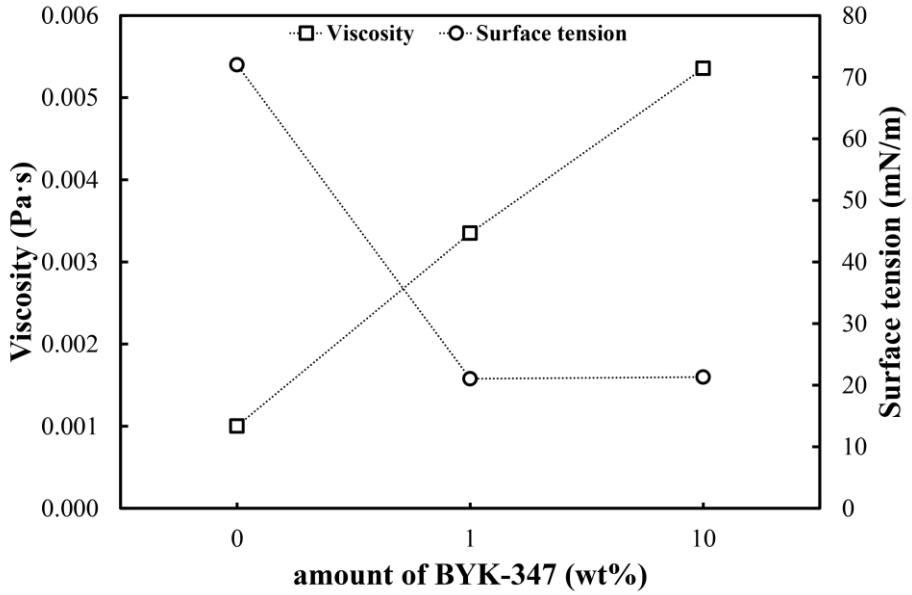

Fig. 3 Variation of water viscosity and water surface tension as a function of the amount of surfactant (BYK–347) added.

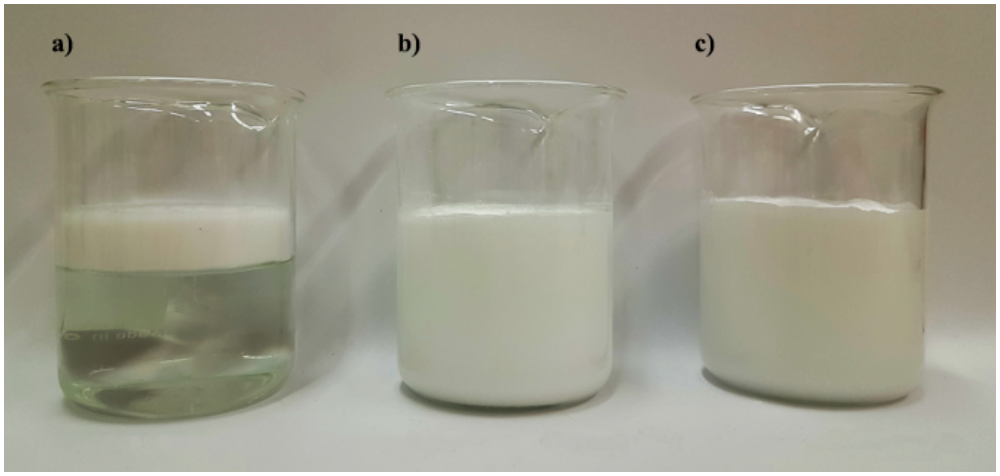

Fig. 4 Appearance of an aqueous suspension of silica aerogel at 25 vol.% solids content a) without the addition of surfactant, b) after the addition of 1wt% surfactant and c) after applying 1 minute of sonication to the suspension.

In addition, Fig. 5 shows the flow curves obtained for the same concentration of solids (25 vol.%) and different sonication times. It can be concluded that the application of sonication to stabilise the aerogel is not beneficial because the shear stress increases when US time goes from 0 to 2 minutes, and consequently the viscosity (ratio between shear stress and shear rate) rises from $12 \cdot 10^{-3}$ Pa·s to $36 \cdot 10^{-3}$ Pa·s, respectively.

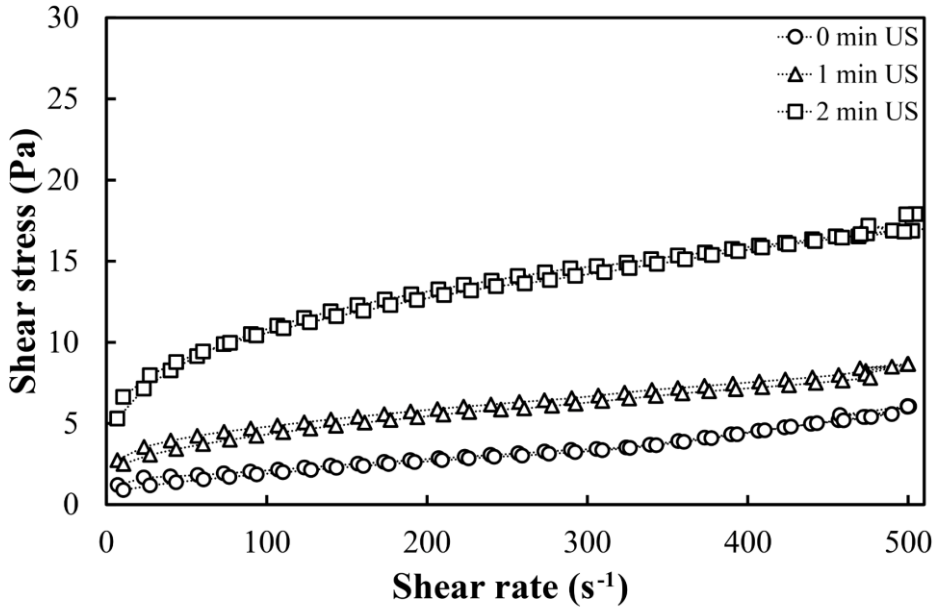

Fig. 5 Flow curves of suspensions at 25 vol.% prepared with silica aerogel for different sonication times.

3.2. Preparation and characterisation of spray–dried powder feedstocks of silica aerogel/Y–TZP mixtures

According to the above results, the same particle concentration (25 vol. %) was chosen for the preparation of the suspensions because it was observed that aerogel could be dispersed. Furthermore, the new suspensions were prepared with variable proportions of zirconia. The addition of zirconia particles should not be a problem because mono and multi component suspensions with high solids content of zirconia particles with low viscosities and good stability have been successfully prepared in a previous work [27,34].

Figure 6 shows the viscosity curves in function of the shear rate of the zirconia suspension and its mixtures with aerogel. The zirconia suspension displays a quasi-Newtonian behaviour with very low viscosities, which are in line with previous research [27,35], while all the samples with silica aerogel particles show a shear-thinning behaviour, which is consistent with results observed above with suspensions containing this material.

Thus, as expected, the shear thinning behaviour increases as the amount of silica particles in the suspension grows. In fact, only the addition of 2 vol. % of aerogel particles to the zirconia suspension converts the quasi-Newtonian behaviour of the suspension into a clearly pseudoplastic behaviour. It can also be observed that the viscosity of the

suspensions at high shear rates increases with the amount of aerogel particles, as a consequence of the extremely high specific surface area of these particles. For the same reason, the presence of aerogel particles gives the suspension a certain thixotropic character which can be deduced from the area of hysteresis enclosed by the viscosity curves. This thixotropy augments with the increase of aerogel content in the suspension and it is clearly visible in contents higher than 30 vol. %. On the other hand, all the suspensions showed sufficient stability (absence of sedimentation and/or agglomeration) over time to ensure an adequate atomisation process.

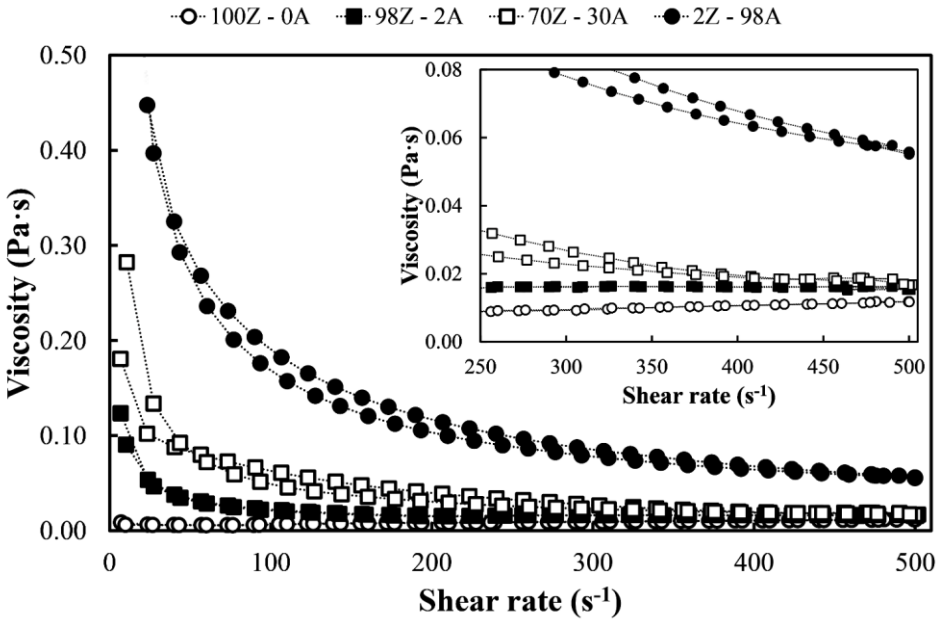

Fig. 6 Viscosity curves as a function of the shear rate of zirconia suspensions and aerogel mixtures with zirconia. For better visualization, the lower part of the graph has been enlarged on the right side of the figure.

Once the rheological behaviour and stability of all the prepared suspensions had been studied, they were atomised in order to obtain reconstituted powders suitable for incorporation into the plasma torch. Table 4 details three agglomerate characteristic diameters which represent the agglomerate size distribution (D_{10}, D_{50} and D_{90}) obtained by image analysis from FEG-ESEM micrographs, while Fig. 7 shows the micrographs of each agglomerated powder in order to appreciate the morphology of the resulting agglomerates.

The results show that only the addition of 2% of aerogel strongly reduces the agglomerate average size and narrows the agglomerate size distribution. The effect is not proportional to aerogel addition since further aerogel amounts hardly affect the distribution characteristics. This reduction in agglomerate size is related to the decrease in surface tension, as a consequence of the surfactant added to promote wetting of the aerogel particles. Hence, the decrease in surface tension gives rise to finer droplet size during atomisation, and therefore smaller agglomerates are obtained. In Fig. 8, the detail of agglomerates in which the zirconia particles tend to coat the aerogel particles can be seen. Fig. 8a shows that for the composition without aerogel, spherical or donut-like agglomerates wrapped in small residual zirconia particles are produced, a morphology characteristic of the atomisation of suspensions. In the compositions with a high amount of zirconia (Fig. 8b y c) zirconia particles homogeneously cover the surface of the aerogel particles. On contrary, when the amount of aerogel prevails over zirconia particles rough agglomerates are produced which are characterised by an expected, deficient coverage of zirconia (Fig. 8d), due to the scarce amount of zirconia present in the composition. Despite this, all the agglomerates obtained are more or less spherical in morphology.

Table 4 Agglomerate size distribution of the agglomerated powders obtained by spray-drying of the studied suspensions.

Coating	**Characteristic agglomerate sizes (µm)**		
	D_{10}	**D_{50}**	**D_{90}**
100Z – 0A	2.0	12.0	45.0
98Z – 2A	2.0	6.0	16.0
70Z – 30A	1.6	5.2	13.0
2Z – 98A	1.6	4.5	12.6

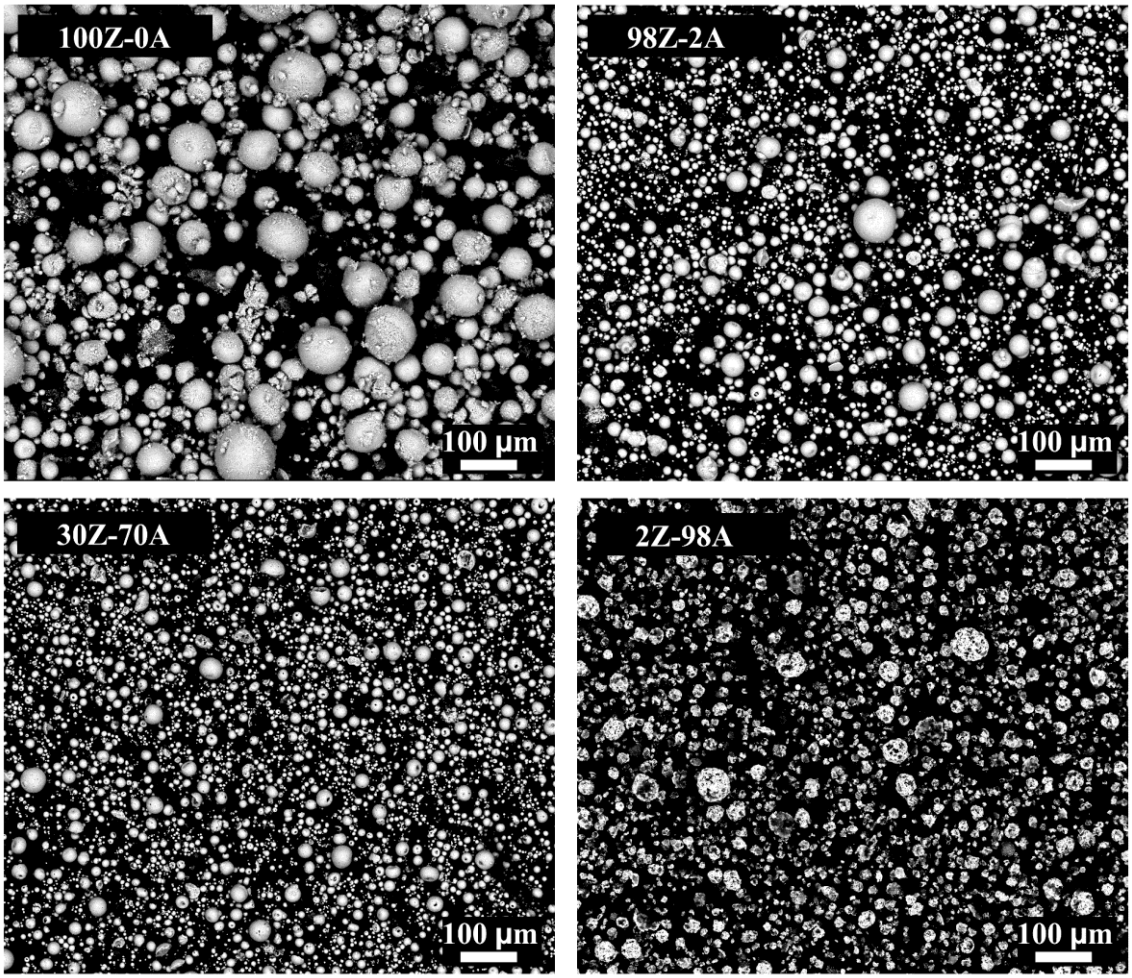

Fig. 7 Micrographs of samples of the atomised powders obtained in the research.

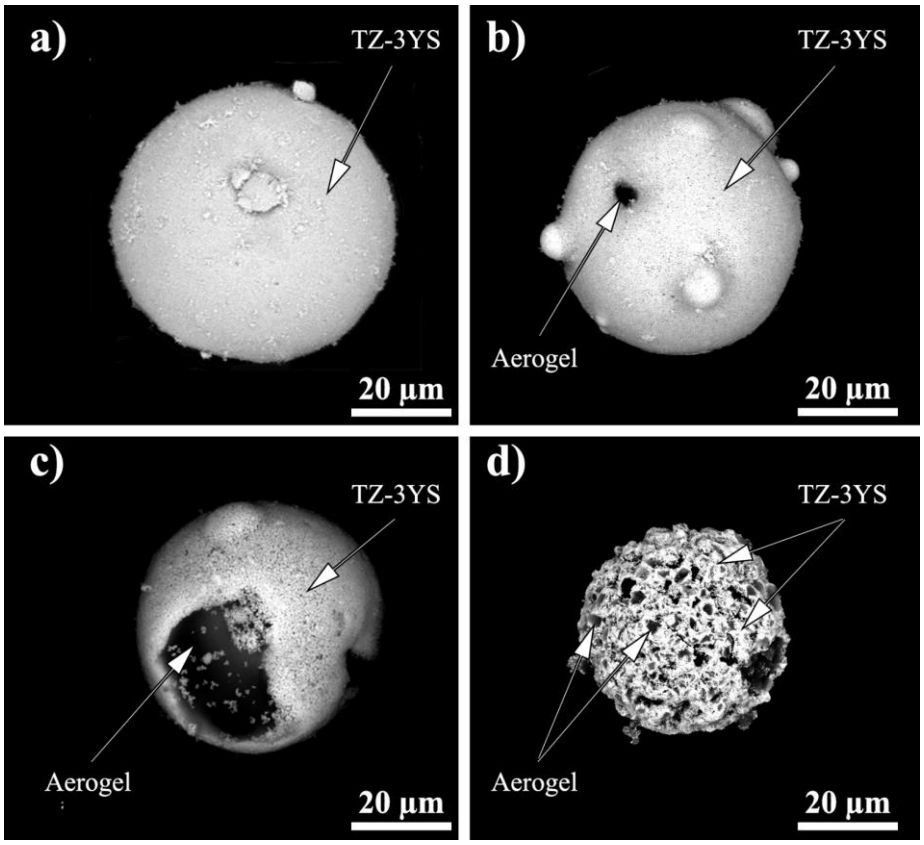

Fig. 8 Detail of the agglomerated powders and the coverage of the zirconia on the aerogel particles. The agglomerated powders correspond to a) 100Z – 0A, b) 98Z – 2A, c) 70Z – 30A and d) 2Z – 98 A.

Fig. 9 shows the rheological behaviour of the powders, which were evaluated by means of the Hausner ratio and angle of repose tests. The Hausner ratio indicates that all powders display good flowability, although, this property is worsened by increasing the addition of aerogel, as a consequence of the decrease of agglomerate size as well as its loss of sphericity as observed in Fig.7 micrographs. Although the angle of repose confirms the good flowability of the four powders, the worsening effect associated to aerogel addition can also be observed. Overall, the four feedstocks possessed quite good flowability, and consequently, all of them are suitable for APS application.

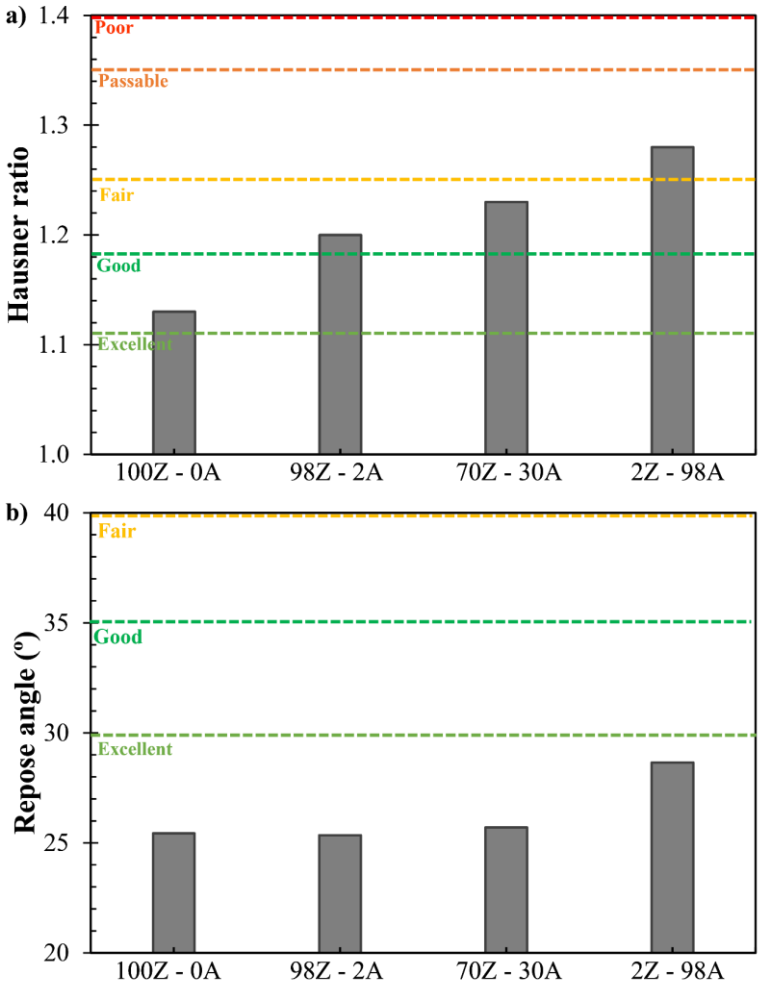

Fig. 9 Flowability of the different agglomerates: a) Hausner ratio test, and b) response angle test. Lines delimiting flowability regions for each test are also included in these plots [30,36].

3.3. Microstructure characterization of coatings

The four agglomerate powders were satisfactorily deposited by plasma spray as set out in cross-sections of Fig. 10. All the coatings are made up of two clearly differentiated layers, i.e the ceramic coating (light layer) and the bond coat (light grey layer) which are deposited on top of the metal substrate (dark grey layer). Besides, the four top coatings display the typical “two-zones” microstructure which results from spraying fine agglomerated powders by APS [37–39]. According to the literature [38], this bimodal microstructure is formed by semi-molten feedstock particles that are surrounded by molten particles that act as a binder to maintain the integrity of the coating. This characteristic is essential in the deposition of submicron or nanostructured coatings and it explains how a certain amount of the initial nanostructure of the feedstock can be

preserved. In the coatings of Fig. 10, the appearance of some areas of unmolten particles (black arrows) indicates that the particles have not fully molten and therefore the probability to preserve aerogel particles with their initial integrity (highly porous) grows. In the coatings 98Z – 2A and 70Z – 30A, it can be seen that there is a large amount of zirconia matrix (practically the whole coatings display light colour) with dispersed aerogel particles as shown by the white arrows. On the other hand, in the 2Z – 98A micrograph a greater presence of aerogel is observed together with zirconia which causes a mixed pattern between light and greyish colours throughout the coating.

Some characteristics of the coatings can be observed in Table 5. The thickness of the coatings is around 110 µm, while the porosity significantly increases with the addition of aerogel. This increase of porosity for the same thermal spray conditions is an expected consequence of the high specific surface area and high porosity of aerogel particles (around 90% porosity). However, the increase in porosity due to the addition of aerogel has a minor impact when compared to the amount of pores in the aerogel particles. Thus, if the aerogel particles would keep their integrity after plasma spraying, a super porous coating would be obtained (i.e., around 88% for 2Z – 98A coating as shown in Table 5), while the actual porosity of the coating reaches only 19%. This difference confirms that aerogel particles do not maintain their integrity during thermal spraying, lose great part of their large porous structure, most likely due to sintering and melting processes as well as possible particle evaporation or sublimation which can occur in the plasma torch due to the extremely high plasma temperatures.

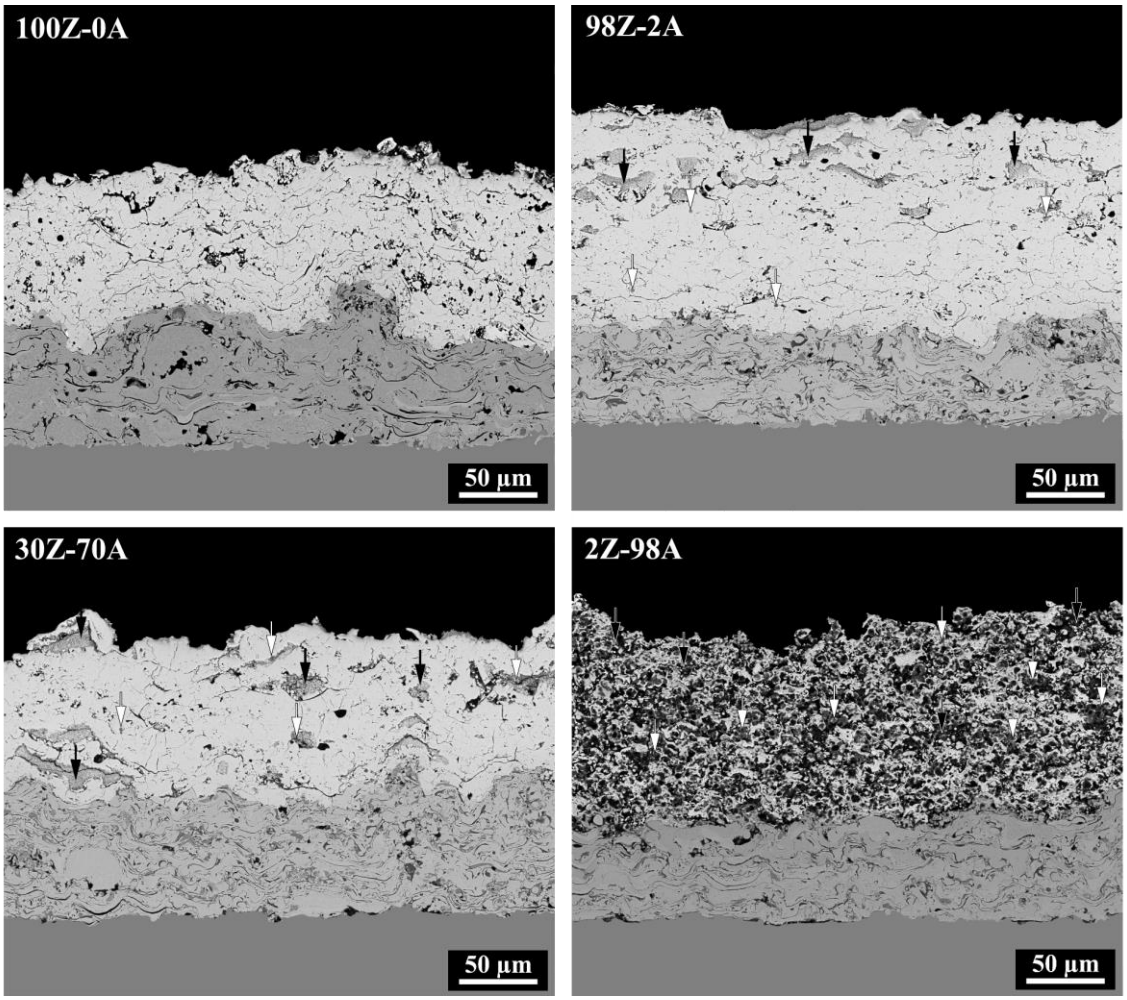

Fig. 10 Detail of the micrographs obtained in cross-section corresponding to the coatings deposited from the four samples tested. Unmolten matrix zones and unmolten aerogel zones are indicated by black and white arrows respectively.

Table 5 Thickness and experimental porosity values obtained by image analysis together with the theoretical porosity values of the coatings.

Coating	Thickness	Experimental porosity	Theoretical porosity*
100Z – 0A	~ 110 µm	5.0	5.0
98Z – 2A		5.3	6.7
70Z – 30A		6.4	30.5
2Z – 98A		19.1	88.3

*Estimated from as-received aerogel particles porosity

A more detailed view of the coatings' microstructure is shown in Fig. 11. The components of the different zones of the coating have been corroborated with EDX analyses as shown in Fig. 12. Thus, in the coatings, i) the black zones are associated with the porosity of the coating, ii) the dark zones refer to the aerogel particles (A) whose shape is similar to that of the initial particles (Fig. 1), iii) the light zones indicate zones with high content of molten zirconium particles (C), iv) the intermediate grey zones refer to a molten mixture of silicon and zirconium (B), which causes the partial loss of the porous properties of the aerogel particle, and which would corroborate the lack of porosity in the coating.

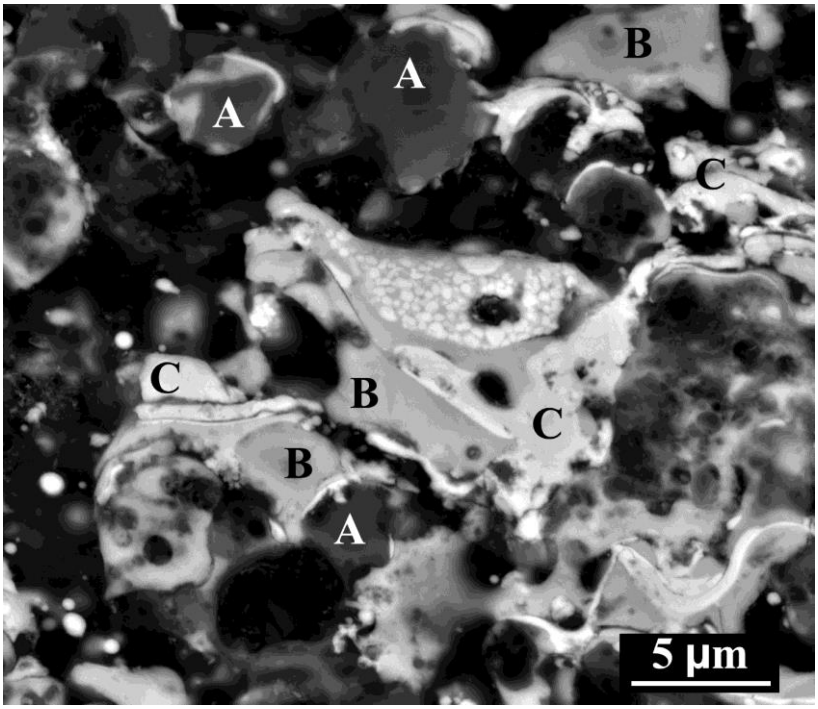

Fig. 11 Detail of the microstructure of 2Z – 98A coating at higher magnification with different zones. The letters A, B and C refer to the zones with high silicon content, a mixture of silicon with zirconia, and high zirconia content respectively.

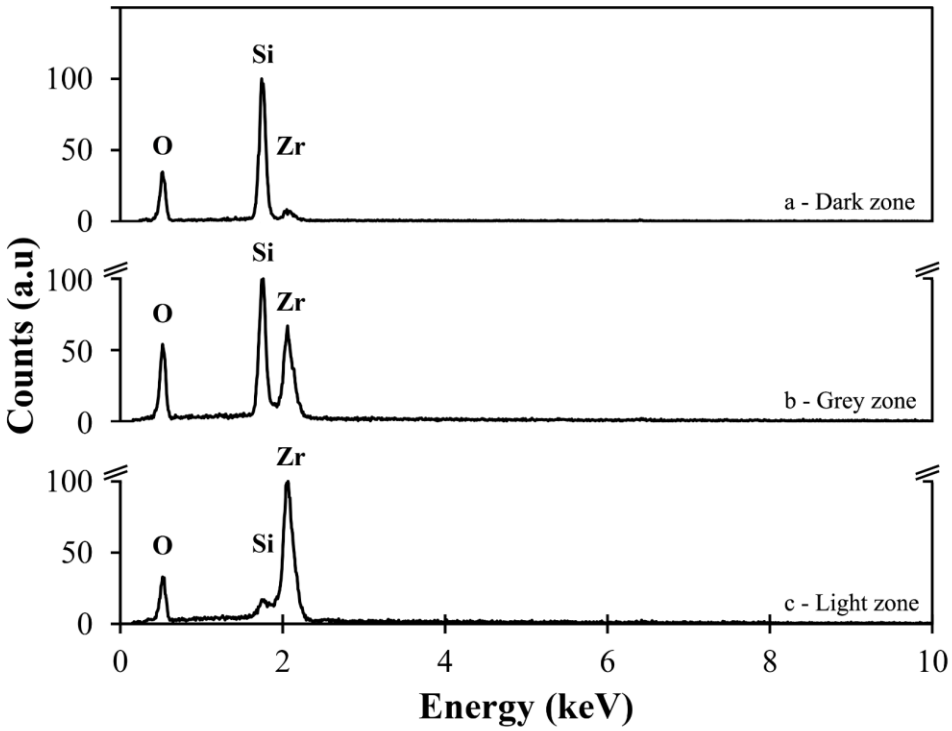

Fig. 12 EDX analysis of different microstructure zones of the 2Z – 98A coating. The letters a, b and c refer to the zones with a high silicon content, a mixture of silicon with zirconia, and a high zirconia content respectively as shown in Fig. 11.

XRD of the coatings of opposite composition (2Z – 98A and 98Z – 2Z) were also carried out to check the possible phases developed during the thermal spraying. The resulting diffraction patterns are shown in Fig. 13, where all the peaks associated to the tetragonal phase of yttria-stabilised zirconia can be visualised, while no further phases which could be related to crystalline silica or zirconia and silica reaction products were identified.

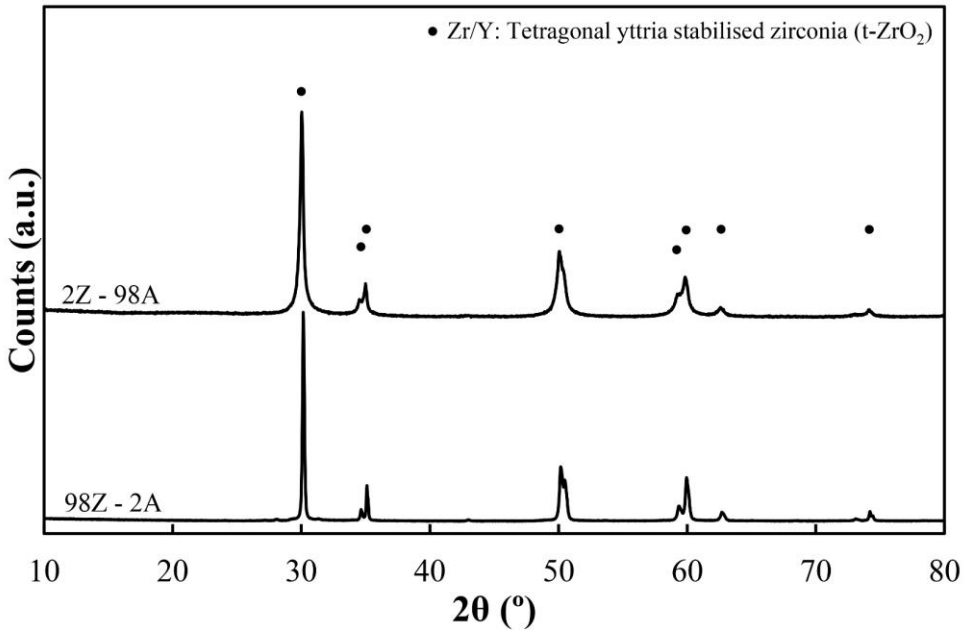

Fig. 13 X-Ray diffractograms of the coatings with 2 and 98 vol.% of aerogel and with zirconia, i.e 2Z – 98A and 2A – 98Z.

To better understand the thermal behaviour of the silica aerogel particles, some experiments in heating microscope (HM 867, TA Instruments) up to 1773 K in air atmosphere were performed. Fig. 14 shows the comparison of micrographs of aerogel particles after this test and after thermal spraying at the conditions used to obtain the coatings. As it can be seen, the sintering process is evident as denoted by particle necking and enlargement. From the heating microscope test it was determined that the sintering of the aerogel particles starts at 1123 K leading to a high shrinkage of about 40%. Concerning the aerogel powder collected after thermal spraying, it can be observed the formation of spherical, clustered particles due to the sintering process, some angular particles are still visible though. Consequently, the sintering process that aerogel particles undergo is one of the reasons for their lower contribution to increasing the final porosity of the coatings.

Another hypothesis related to the lower porosity contribution of aerogel particles in comparison to the theoretical, expected contribution was the possibility of losing silica particles due to sublimation. Therefore, in order to determine the amount of silica in the final coatings, a chemical analysis of sample 70Z – 30A by FRX was performed, and the results are shown in Table 6. Thus, only 0.5% in weight of silica was determined with

the chemical analysis with respect to the 0.9% in weight of initial silica (which corresponds to 30 % volume of aerogel). This finding confirms that a significant part of the aerogel melts and then evaporates or directly sublimates during thermal spraying (about 44%), which corroborates what was observed in the cross-section micrographs (Fig. 10) and porosity values (Table 5), where the microstructure of the coating does not undergo a substantial modification until high aerogel contents (98 vol.%) are incorporated. The other components observed in chemical analysis, such as zirconia or yttria, are within the expected range because of their high melting point. Other oxides were also observed in smaller proportions from possible contamination during powder collection.

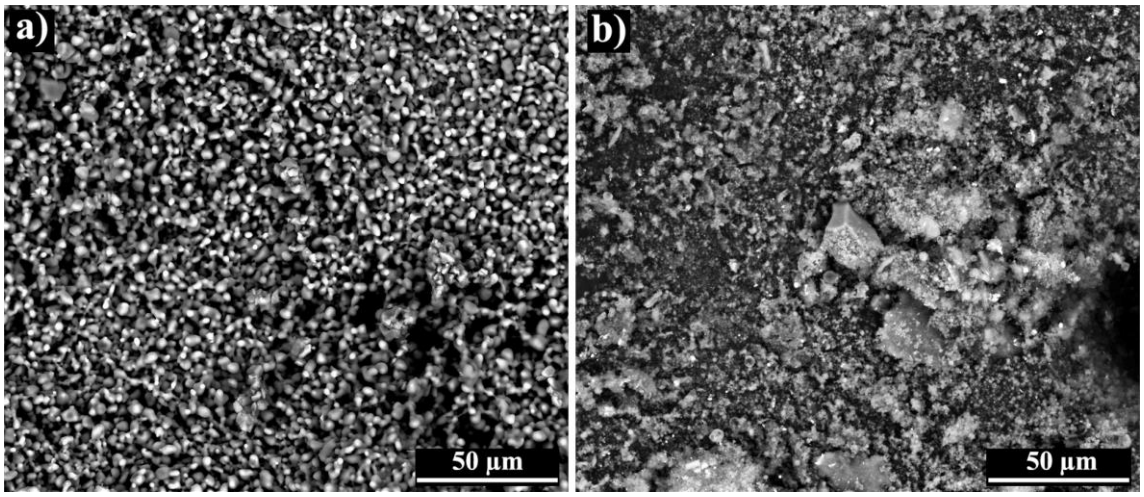

Fig. 14 Comparison of aerogel particles to different thermal treatments to observe the state and thermal behaviour of the particles, a) heating microscopy at 1773 K, and b) thermal spraying of powders.

Table 6 Chemical analysis by FRX of the powder sprayed from composition 70Z – 30A.

Oxides	**% Weight**
ZrO_2	92.2
SiO_2	0.5
Y_2O_3	5.6
Others	1.7

3.4 Thermal conductivity of coatings

Finally, the variation in thermal conductivity was determined from the measurement of thermal diffusivity, specific heat and apparent density of the coatings, as indicated in the experimental section. Average values of experimental specific heat of the powers were as follows: 0.551 and 0.405 J/g·K for TZ – 3YS and aerogel particles, respectively. In all the cases, the obtained average values are consistent with those reported in the literature [40,41]. From these values, calculations of the specific heat of the compositions were carried out by the mixing rule with the following average values: 0.552, 0.550, 0.507 and 0.406 J/g·K for the 100Z, 98Z – 2A, 70Z – 30A and 2Z – 98A coatings, respectively.

Fig. 15 shows the thermal conductivity of the coatings versus temperature. The trend of thermal conductivity for all curves shows a very similar profile: a strong decrease up to 673K, then a moderate decrease down to values around 1 W/m·K and finally a stabilization to reach values below 0.75 W/m·K at maximum temperatures. It can be seen that the addition of aerogel is beneficial to reduce the thermal conductivity in any proportion, although the decrease is not proportional to the percentage of aerogel added, as shown in the Table 7. However, very low thermal conductivities can be achieved with high aerogel additions, as observed in the 2Z – 98A ratio, which presents an evident morphological change in the coating (e.g., high porosity) that together with the characteristics of the aerogel particles favour this large decrease. In addition, it can be observed that the material over cost for the addition of aerogel is not very high (up to 98 vol.%) and a good reduction of the thermal conductivity is achieved, so that, a priori, the design of TBCs coatings by using silica aerogel particles could be feasible. These coatings could be engineered from mixtures of zirconia-aerogel particles in multilayer or functionally graded structures.

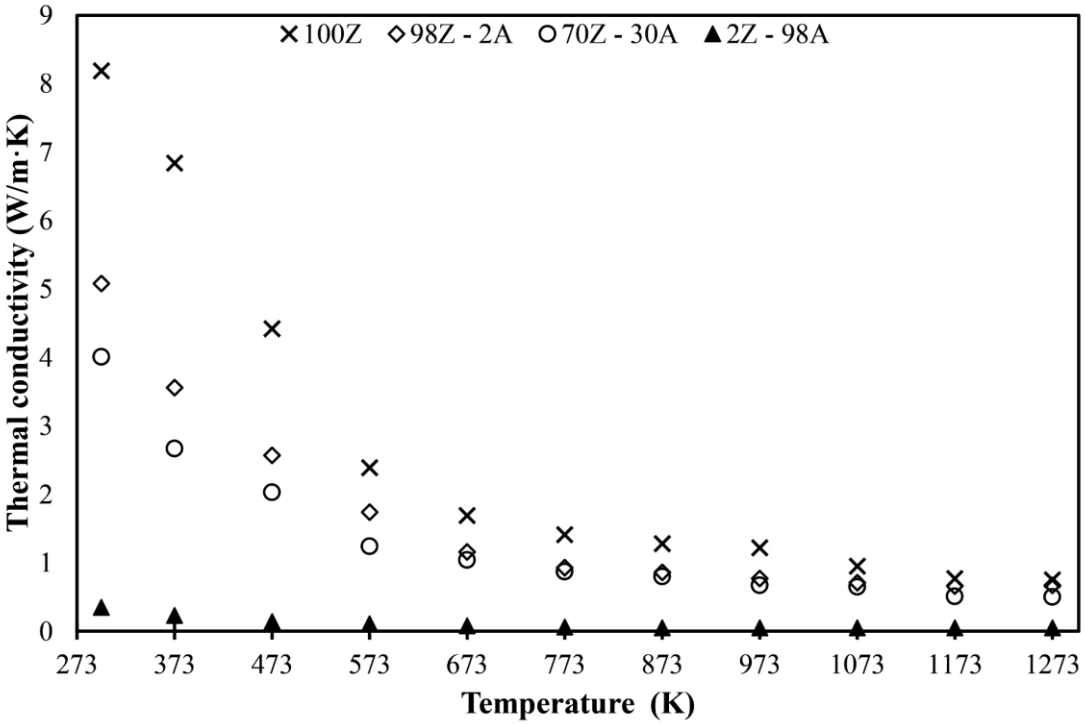

Fig. 15 Plot of thermal conductivity as a function of temperature for the four coatings obtained by atmospheric plasma spraying.

Table 7 Effectiveness of aerogel addition on thermal conductivity and cost overrun in the production of thermal barrier coatings.

	Thermal conductivity (at 1000ºC)	**TC reduction[1] (%)**	**Addition of aerogel (%) (volume/weight)**	**Cost overruns[2] (%)**
100 Z	0.75	0.0	0 / 0	0.0
98Z – 2A	0.67	10.6	2 / 0.01	0.2
70Z – 30A	0.50	33.3	30 / 0.9	0.8
2Z – 98A	0.05	93.3	98 / 52	21.3

(1) TC reduction: Thermal conductivity reduction

(2) Overcost of suspension in relation to the amount of raw material employed (only the cost of powders is considered).

4. Conclusions

The incorporation of silica aerogel particles in zirconia ceramic coatings obtained by plasma spraying has been explored in this research. Amounts of silica aerogel addition to zirconia powder ranging from 2% to 98% (vol.%) have been addressed. However, some limitations appear due to the difficulty in dispersing the aerogel particles in an aqueous medium as a consequence of the extremely high hydrophobicity and specific surface area of this powder. The following conclusions can be then drawn: i) With a rheological adaptation and including a surfactant it is possible to disperse highly hydrophobic aerogel particles in water to obtain concentrated suspensions. ii) A valid methodology was achieved to prepare concentrated suspensions of zirconia and aerogel particles in different proportions and to subsequently atomise them satisfactorily to obtain spray-dried powders. iii) The agglomerated powders display a good morphology and size distribution that give them suitable flowability. Although the addition of aerogel slightly worsens this flowability, all powders exhibit suitable characteristics to be fed into the plasma torch. iv) The coatings obtained by plasma spraying display similar thickness, but the addition of aerogel increases the porosity, as a consequence of the inner porosity and specific surface area of aerogel particles. v) The microstructural characterisation of the coatings and powder samples confirms that part of the aerogel particles sinter and melt, a significant amount of the particles disappear as a result of evaporation or sublimation~~,~~ while others remain integrated in the matrix of the coating without forming other phases with zirconia. Crystallisation of silica phases was not observed. vi) The addition of aerogel in the coatings had beneficial effects in the reduction of the thermal conductivity of the coatings with a high feasibility due to its affordable cost.

Acknowledgements

The authors of this study thank Universitat Jaume I of Castellon for the support provided in funding the AEROPLASMA project (UJI–B2017–77) and Spanish Ministry of Science, Innovation and Universities (MCIU), the State Research Agency (AEI) and the European Regional Development Fund (FEDER) for the support provided in funding the ACCESO project (RTI2018–099033–B–C31). V. Carnicer thanks the Research Promotion Plan of the University Jaume I for the predoctoral fellowship (re. PREDOC/2017/51).

References

[1] N. Espallargas, Future Development of Thermal Spray Coatings: Types, Designs, Manufacture and Applications, Woodhead publishing, 2015. doi:10.1016/B978-0-85709-769-9.00011-7.

[2] A. Vardelle, C. Moreau, J. Akedo, H. Ashrafizadeh, C.C. Berndt, J.O. Berghaus, M. Boulos, J. Brogan, A.C. Bourtsalas, A. Dolatabadi, M. Dorfman, T.J. Eden, P. Fauchais, G. Fisher, F. Gaertner, M. Gindrat, R. Henne, M. Hyland, E. Irissou, E.H. Jordan, K.A. Khor, A. Killinger, Y.-C. Lau, C.-J. Li, L. Li, J. Longtin, N. Markocsan, P.J. Masset, J. Matejicek, G. Mauer, A. McDonald, J. Mostaghimi, S. Sampath, G. Schiller, K. Shinoda, M.F. Smith, A.A. Syed, N.J. Themelis, F.-L. Toma, J.P. Trelles, R. Vassen, P. Vuoristo, The 2016 Thermal Spray Roadmap, J. Therm. Spray Technol. 25 (2016) 1376–1440. doi:10.1007/s11666-016-0473-x.

[3] N.P. Padture, Thermal Barrier Coatings for Gas-Turbine Engine Applications, Science (80-.). 296 (2002) 280–284. doi:10.1126/science.1068609.

[4] R. Vassen, M.O. Jarligo, T. Steinke, D.E. Mack, D. Stöver, Overview on advanced thermal barrier coatings, Surf. Coatings Technol. 205 (2010) 938–942. doi:10.1016/j.surfcoat.2010.08.151.

[5] D.R. Clarke, Materials selection guidelines for low thermal conductivity thermal barrier coatings, Surf. Coatings Technol. 163–164 (2003) 67–74. doi:https://doi.org/10.1016/S0257-8972(02)00593-5.

[6] X.Q. Cao, R. Vassen, D. Stoever, Ceramic materials for thermal barrier coatings, J. Eur. Ceram. Soc. 24 (2004) 1–10. doi:10.1016/S0955-2219(03)00129-8.

[7] R. Vassen, X. Cao, F. Tietz, D. Basu, D. Stöver, Zirconates as New Materials for Thermal Barrier Coatings, J. Am. Ceram. Soc. 83 (2004) 2023–2028. doi:10.1111/j.1151-2916.2000.tb01506.x.

[8] E. Bakan, R. Vassen, Ceramic top coats of plasma-sprayed thermal barrier coatings: materials, processes, and properties, J. Therm. Spray Technol. 26 (2017) 992–1010. doi:10.1007/s11666-017-0597-7.

[9] W. Fan, Y. Bai, Review of suspension and solution precursor plasma sprayed thermal barrier coatings, Ceram. Int. 42 (2016) 14299–14312. doi:10.1016/J.CERAMINT.2016.06.063.

[10] A. Ganvir, N. Curry, S. Govindarajan, N. Markocsan, Characterization of Thermal Barrier Coatings Produced by Various Thermal Spray Techniques Using Solid Powder, Suspension, and Solution Precursor Feedstock Material, Int. J. Appl. Ceram. Technol. 13 (2016) 324–332. doi:10.1111/ijac.12472.

[11] V. Stathopoulos, V. Sadykov, S. Pavlova, Y. Bespalko, Y. Fedorova, L. Bobrova, A. Salanov, A. Ishchenko, V. Stoyanovsky, T. Larina, V. Ulianitsky, Z. Vinokurov, V. Kriventsov, Design of functionally graded multilayer thermal barrier coatings for gas turbine application, Surf. Coatings Technol. 295 (2016) 20–28. doi:10.1016/j.surfcoat.2015.11.054.

[12] F. Kirbiyik, M.G. Gok, G. Goller, Microstructural, mechanical and thermal properties of Al 2 O 3 /CYSZ functionally graded thermal barrier coatings, Surf. Coatings Technol. 329 (2017) 193–201. doi:10.1016/j.surfcoat.2017.08.025.

[13] Y. Chen, X. Zhang, S. van der Zwaag, W.G. Sloof, P. Xiao, Damage evolution in a self-healing air plasma sprayed thermal barrier coating containing self-shielding MoSi 2 particles, J. Am. Ceram. Soc. 102 (2019) 4899–4910. doi:10.1111/jace.16313.

[14] V. Carnicer, M.J. Orts, R. Moreno, E. Sánchez, Microstructure assessment of suspension plasma spraying coatings from multicomponent submicronic Y-TZP/Al_2O_3/SiC particles, Ceram. Int. 44 (2018) 12014–12020. doi:10.1016/j.ceramint.2018.03.186.

[15] J. Fricke, Aerogels — highly tenuous solids with fascinating properties, J. Non. Cryst. Solids. 100 (1988) 169–173. doi:10.1016/0022-3093(88)90014-2.

[16] J. Fricke, A. Emmerling, Aerogels, J. Am. Ceram. Soc. 75 (1992) 2027–2035. doi:10.1111/j.1151-2916.1992.tb04461.x.

[17] G.S. Kim, S.H. Hyun, H.H. Park, Synthesis of Low-Dielectric Silica Aerogel Films by

Ambient Drying, J. Am. Ceram. Soc. 84 (2004) 453–55. doi:10.1111/j.1151-2916.2001.tb00677.x.
[18] J. Schultz, K. Jensen, F. Kristiansen, Super insulating aerogel glazing, Sol. Energy Mater. Sol. Cells. 89 (2005) 275–285. doi:10.1016/j.solmat.2005.01.016.
[19] C.E. Carraher, Silica aerogels - properties and uses, Polym. News. 30 (2005) 386–388. doi:10.1080/00323910500402961.
[20] L.W. Hrubesh, Aerogel applications, J. Non. Cryst. Solids. 225 (1998) 335–342. doi:10.1016/S0022-3093(98)00135-5.
[21] M. Schmidt, F. Schwertfeger, Applications for silica aerogel products, J. Non. Cryst. Solids. 225 (1998) 364–368. doi:10.1016/S0022-3093(98)00054-4.
[22] A. Soleimani Dorcheh, M.H. Abbasi, Silica aerogel; synthesis, properties and characterization, J. Mater. Process. Technol. 199 (2008) 10–26. doi:10.1016/j.jmatprotec.2007.10.060.
[23] H. Maleki, L. Durães, A. Portugal, An overview on silica aerogels synthesis and different mechanical reinforcing strategies, J. Non. Cryst. Solids. 385 (2014) 55–74. doi:10.1016/j.jnoncrysol.2013.10.017.
[24] N. Bheekhun, A.R.A. Talib, S. Mustapha, R. Ibrahim, M.R. Hassan, Towards an aerogel-based coating for aerospace applications: reconstituting aerogel particles via spray drying, IOP Conf. Ser. Mater. Sci. Eng. 152 (2016) 012066. doi:10.1088/1757-899X/152/1/012066.
[25] I.S.M. Zulkifli, M.A.M. Yajid, H. Hamdan, M.N.M. Muhid, Maerogel: Alternative for Thermal Barrier Coating Topcoat, Adv. Mater. Res. 845 (2013) 330–334. doi:10.4028/www.scientific.net/AMR.845.330.
[26] I. Syaqirah, M. Zulkifli, M. Azizi, M. Yajid, M.H. Idris, H. Hamdan, Granulation of Maerogel with Solid Sphere Soda-Lime and Boro-Silicate Glass Powder by Using Spray-Drying Process, Aust. J. Basic Appl. Sci. 8 (2014) 313–318.
[27] V. Carnicer, C. Alcazar, E. Sánchez, R. Moreno, Aqueous suspension processing of multicomponent submicronic Y-TZP/Al_2O_3/SiC particles for suspension plasma spraying, J. Eur. Ceram. Soc. 38 (2018) 2430–2439. doi:10.1016/j.jeurceramsoc.2018.01.006.
[28] A.C.-Y. Wong, Use of angle of repose and bulk densities for powder characterization and the prediction of minimum fluidization and minimum bubbling velocities, Chem. Eng. Sci. 57 (2002) 2635–2640. doi:10.1016/S0009-2509(02)00150-1.
[29] M. Vicent, E. Bannier, R. Benavente, M.D. Salvador, T. Molina, R. Moreno, E. Sánchez, Influence of the feedstock characteristics on the microstructure and properties of Al2O3–TiO2 plasma-sprayed coatings, Surf. Coatings Technol. 220 (2013) 74–79. doi:10.1016/j.surfcoat.2012.09.042.
[30] R. Soldati, C. Zanelli, G. Guarini, S. Fazio, M.C. Bignozzi, M. Dondi, Characteristics and rheological behaviour of spray-dried powders for porcelain stoneware slabs, J. Eur. Ceram. Soc. 38 (2018) 4118–4126. doi:10.1016/j.jeurceramsoc.2018.04.042.
[31] P. Carpio, E. Bannier, M.D. Salvador, R. Benavente, E. Sánchez, Multilayer and Particle Size-Graded YSZ Coatings Obtained by Plasma Spraying of Micro- and Nanostructured Feedstocks, J. Therm. Spray Technol. 23 (2014) 1362–1372. doi:10.1007/s11666-014-0143-9.
[32] P. Carpio, R. Moreno, A. Gómez, M.D. Salvador, E. Sánchez, Role of suspension preparation in the spray drying process to obtain nano/submicrostructured YSZ powders for atmospheric plasma spraying, J. Eur. Ceram. Soc. 35 (2015) 237–247. doi:10.1016/j.jeurceramsoc.2014.08.008.
[33] V. Carnicer, F. Martinez-Julian, M.J. Orts, E. Sánchez, R. Moreno, Effect of fructose-containing feedstocks on the microstructure of multicomponent coatings deposited by suspension plasma spraying, J. Eur. Ceram. Soc. 39 (2019). doi:10.1016/j.jeurceramsoc.2019.04.042.
[34] V. Carnicer, M.J. Orts, R. Moreno, E. Sánchez, Influence of solids concentration on the microstructure of suspension plasma sprayed Y-TZP/Al_2O_3/SiC composite coatings, Surf. Coatings Technol. 371 (2019) 143–150. doi:10.1016/j.surfcoat.2019.01.078.
[35] V. Carnicer, C. Alcázar, M.J. Orts, E. Sánchez, R. Moreno, Microfluidic rheology: A new

approach to measure viscosity of ceramic suspensions at extremely high shear rates, Open Ceram. 5 (2021) 100052. doi:10.1016/j.oceram.2020.100052.
[36] A.P. Gorle, S.S. Chopade, Liquisolid Technology: Preparation, Characterization and Applications, J. Drug Deliv. Ther. 10 (2020) 295–307. doi:10.22270/jddt.v10i3-s.4067.
[37] R.S. Lima, B.R. Marple, Nanostructured YSZ thermal barrier coatings engineered to counteract sintering effects, Mater. Sci. Eng. A. 485 (2008) 182–193. doi:10.1016/j.msea.2007.07.082.
[38] R.S. Lima, B.R. Marple, Thermal spray coatings engineered from nanostructured ceramic agglomerated powders for structural, thermal barrier and biomedical applications: A review, J. Therm. Spray Technol. 16 (2007) 40–63. doi:10.1007/s11666-006-9010-7.
[39] P. Fogarassy, D. Gerday, A. Lodini, Agglomerated nanostructured particles disintegration during the plasma thermal spraying process, Mech. Res. Commun. 32 (2005) 221–239. doi:https://doi.org/10.1016/j.mechrescom.2004.05.007.
[40] P. Sokołowski, S. Björklund, R. Musalek, R.T. Candidato, L. Pawłowski, B. Nait-Ali, D. Smith, Thermophysical properties of YSZ and YCeSZ suspension plasma sprayed coatings having different microstructures, Surf. Coatings Technol. 318 (2017) 28–38. doi:10.1016/j.surfcoat.2017.02.054.
[41] F. Yang, X. Zhao, P. Xiao, Thermal conductivities of YSZ/Al2O3 composites, J. Eur. Ceram. Soc. 30 (2010) 3111–3116. doi:https://doi.org/10.1016/j.jeurceramsoc.2010.07.007.